INRIA

UNITÉ DE RECHERCHE
INRIA-SOPHIA ANTIPOLIS

Institut National
de Recherche
en Informatique
et en Automatique

Domaine de Voluceau
Rocquencourt
B.P.105
78153 Le Chesnay Cedex
France
Tél. (1) 39 63 55 11

Rapports de Recherche

N° 1338

Programme 6
Robotique, Image et Vision

IMAGE SEGMENTATION USING 4 DIRECTION LINE-PROCESSES

Josiane ZERUBIA
Davi GEIGER

Décembre 1990

RR-1338

Programme 6

IMAGE SEGMENTATION USING 4 DIRECTION LINE-PROCESSES

SEGMENTATION D'IMAGE UTILISANT DES PROCESSUS DE LIGNE DANS 4 DIRECTIONS

Josiane ZERUBIA[1] Davi GEIGER[2]

1. INRIA - Sophia Antipolis - 2004 route des lucioles - 06560 Valbonne - FRANCE.

2. Siemens Corporate Research Inc., 755 College East Road - Princeton - NJ08540 - USA.

November 1990

abstract

In recent years, many researchers have investigated the use of Markov Random Fields (MRF)for early vision. This type of modelization can be applied to several problems such as edge detection, image restoration, stereo vision, long-range motion and so on.

In this paper, we present a new model using line-processes in 4 directions in order to have a better detection of diagonal lines and curves. A deterministic relaxation algorithm using Mean Field Annealing (MFA) is derived which gives the mean values of the intensity fields and the 4 direction line-processes. Finally, a winner-take-all scheme is proposed to select the edges. Furthermore, we show how we propagate the lines at low temperatures including an additional constraint in the cost (or energy) function. Then, we present simulation results obtained on real images with a connection machine CM2 using an optimal step descent technique to minimize the cost. We compare these results to those obtained with an algorithm previously proposed and which only deals with horizontal and vertical line-processes.

résumé

Dernièrement, de nombreux chercheurs ont utilisé des champs de Markov en vision bas-niveau. Ce type de modélisation peut être appliqué à divers problémes tels que la détection de contours, la restauration d'image, la vision stéréoscopique, le mouvement etc...

Dans ce papier, nous présentons un nouveau modéle qui utilise des processus de ligne dans 4 directions afin d'obtenir une meilleure détection des diagonales et des courbes. Un algorithme déterministe de relaxation faisant appel au recuit par champs moyens est proposé. Il donne la valeur moyenne du champ intensité et des processus de ligne dans les 4 directions. Enfin, un algorithme de type "winner-take-all" est proposé pour détecter les contours. De plus, nous montrons comment effectuer une propagation des lignes à basse température grâce à l'addition d'une contrainte dans la fonction coût (ou énergie). Puis, nous présentons des résultats de simulation obtenus à partir d'images réelles sur une machine à connections CM2 avec un algorithme de descente optimale pour minimiser le coût. Nous comparons ces résultats à ceux obtenus par un algorithme proposé précédemment et qui ne fait appel qu'à des processus de ligne horizontaux et verticaux.

key words

Markov Random Fields,deterministic relaxation, edge detection.

mots clefs

Champs de Markov, relaxation déterministe, détection de contours.

Contents

1 Introduction :

In early vision, Markov Random Field (MRF) modelization [15] and regularization theory [24] has received a great deal of attention in the last few years [9],[17],[21],[28]. Usually two fields are coupled to represent the image : one is dedicated to the intensity values, the other one is used to model the discontinuities through the line-processes. This type of modelization, originally introduced in vision by Geman and Geman [11], has been widely used for edge detection [25],[26],[27],[36],[37], image restoration [10],[11],[14], stereovision [33], surface reconstruction [3],[4],[7],[8], long range motion [32] and so on.

For all these early vision processes, the problem is posed as one of minimizing a cost function which is derived from the negative logarithm of an appropriate posterior probablity density function, which can be tought as the length of encoding. The cost function obtained is non-convex due to the line-processes and several relaxation techniques have been proposed to reach the global minimum. The first group of methods deals with stochastic relaxation and is based on simulated annealing [11],[14],[16],[30]. These algorithms converge asymptotically towards the global minimum but require a great deal of computation. The second group of methods is related to deterministic relaxation. These techniques are suboptimal but require less computational time than the previous ones. This is why so many deterministic relaxation algorithms have been recently investigated (Graduated Non Convexity (GNC) [3],[4],[25].[27], Iterated Conditional Mode (ICM) [1],[14], Mean Field Annealing (MFA) [6],[8].[20].[33].[34].[36]. [37])

In this paper, we present a model based on MRF using line-processes in 4 directions in order to have a better detection of diagonal lines and curves. A deterministic relaxation algorithm using MFA is derived which gives the mean values of the intensity fields and the 4 direction line-processes. Finally, a winner-take-all scheme is proposed to select the edges. Furthermore, we show how we propagate the lines at low temperatures including an additional constraint in the energy function.

The plan of this paper is as follows : in Section 2, we review the two line-process (horizontal and vertical line-process) model and the use of the mean field techniques including the winner-take-all scheme. The case of an anisotropic model is also considered [36],[37]. Section 3 is dedicated to the new model with 4 direction line-processes and gives a set of iterative equations to get the mean values of the fields. In Section 4, we propose an extension of the model to propagate lines. In Section 5, we present the simulation results obtained with a connection machine CM2 on real images using an optimal step descent method to minimize the cost function. Finally, we compare these results to those obtained with the previous model and conclude.

2 Two line-process model and mean field techniques:

2.1 Previous model with horizontal and vertical line-processes :

The weak membrane model can be derived from Bayes theory considering the model for the noise to be Gaussian and a prior distribution for the image to be a piecewise smooth function. In two dimension, it is represented by the following cost function (or energy) [4],[11] :

$$E(y,h,v) = \sum_{i,j}[(y_{i,j} - d_{i,j})^2 + \alpha(\Delta^h_{i,j}{}^2(1 - h_{i,j}) + \Delta^v_{i,j}{}^2(1 - v_{i,j})) + \gamma(h_{i,j} + v_{i,j})] \quad (1)$$

where $(d_{i,j})$ are the observed data, α is a smoothing parameter, γ is a penalty parameter to create an edge, $h_{i,j}$ is the horizontal line-process which connects the site(i,j) to the site(i,j-1) and $v_{i,j}$ the vertical one which connects the site(i,j) to the site(i-1,j) (see Fig. 1), and $\Delta^h_{i,j}$ and $\Delta^v_{i,j}$ are the gradient in each direction given by :

$$\Delta^h_{i,j} = y_{i,j} - y_{i-1,j} \quad (2)$$

$$\Delta^v_{i,j} = y_{i,j} - y_{i,j-1} \quad (3)$$

The first term in the energy enforces closeness to the data, the second one corresponds to the regularization term which results in a smoothing, the third one takes into account the price to be paid to create an edge.

Through Hammersley-Clifford theorem, this energy function is related to the probability of a given solution for the fields by the Gibbs distribution [22]:

$$P(y,l) = \frac{\exp -\beta E(y,l)}{Z} \quad (4)$$

which means that every state of the system has a finite probability to occur (the more likely states being those with the lowest energy). In this case the fields y and l are coupled Markov Random Fields. As the temperature goes to zero (i.e. β tends to infinity), the solution converges to the most probable one.

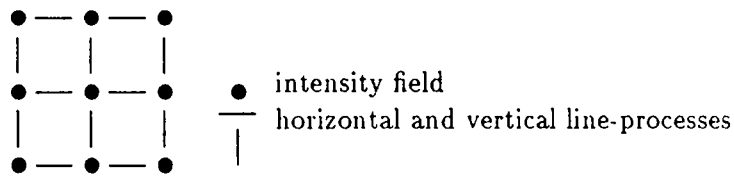

Figure 1: MRF model with horizontal and vertical line-processes

2.2 Mean Field approximation :

Using results from statistical mechanics [22],[23], it can be shown [7],[8] that it is possible, under some conditions. to compute a good approximate solution from the partition function Z defined by :

$$Z = \sum_{all\ configurations} \exp -\beta E(y, l) \tag{5}$$

using Mean Field (MF) approximation. This approximation consists of replacing the stochastic interaction among the fields at different locations by the interaction of the field at each site with the mean field values at different locations. Once the partition function Z is known, it is easy to derive a set of deterministic equations for the mean field values $\bar{y}$ and $\bar{l}$ of the intensity and the line-process [7],[8]. These values are the minimum variance estimators for the fields and converge to a minimum at zero temperature [6],[32].

MF approximation has also been widely used in other fields such as neural networks for instance because it gives a good approximation of the solution and reaches an equilibrium state at a given temperature much faster than simulated annealing [2].[5].[12].

2.3 Mean Field and the two line-processes :

Using MF approximation, the following set of deterministic equations is derived (see [7] and [8] for more details) :

$$\begin{aligned}\bar{y}_{i,j} &= d_{i,j} - \alpha\Delta^{\bar{v}}_{i,j}(1-\bar{v}_{i,j}) + \alpha\Delta^{\bar{v}}_{i,j+1}(1-\bar{v}_{i,j+1}) \\ &\quad - \alpha\Delta^{\bar{h}}_{i,j}(1-\bar{h}_{i,j}) + \alpha\Delta^{\bar{h}}_{i+1,j}(1-\bar{h}_{i+1,j})\end{aligned} \tag{6}$$

$$\bar{h}_{i,j} = \sigma_\beta(\alpha{\Delta^{\bar{h}}_{i,j}}^2 - \gamma) \tag{7}$$

$$\bar{v}_{i,j} = \sigma_\beta(\alpha{\Delta^{\bar{v}}_{i,j}}^2 - \gamma) \tag{8}$$

$$\Delta^{\bar{h}}_{i,j} = \bar{y}_{i,j} - \bar{y}_{i-1,j} \tag{9}$$

$$\Delta^{\bar{v}}_{i,j} = \bar{y}_{i,j} - \bar{y}_{i,j-1} \tag{10}$$

where σ_β is the sigmoid function :

$$\sigma_\beta(u) = \frac{1}{1+\exp -\beta u} \tag{11}$$

In order to enforce the smoothness of the discontinuity field (i.e. the line-process), an additional constraint can be incorporated in the model by adding a new term in the energy function :

$$E^{new}(y,h,v) = E(y,h,v) - \epsilon\gamma\sum_{i,j}[h_{i,j}\frac{h_{i,j-1}+h_{i,j+1}}{2} + v_{i,j}\frac{v_{i-1,j}+v_{i+1,j}}{2}] \tag{12}$$

so that the presence of a discontinuity at a site makes more likely the presence of a discontinuity at a neighboring site (see [8] for more details).

Another possibility is to use an anisotropic MRF [36],[37] instead of the isotropic model presented above. This model is better for image restoration eventhough it involves more computation to estimate the MRF parameters (see [36] for more details). But when the goal is only edge detection, the isotropic model is sufficient.

2.4 Winner-take-all :

The winner-take-all scheme can be defined as follows : given a set of N inputs to a system, we want to get the maximum input and suppress the others. To solve this problem,

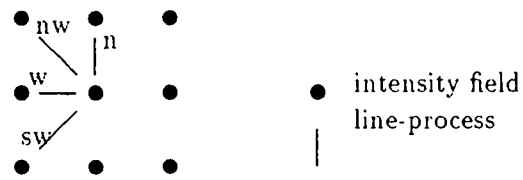

Figure 2: A model with 4 direction line-processes

two methods are available (see [6], [32] for more details) : the constraint of having only one winner is imposed either by adding a term in the energy function to bias towards final states with a single winner using mean field approximation, or by evaluating the partition function for the system only over configurations with a single winner which gives an exact solution. The winner-take-all scheme can be used in vision to perform non-maximum suppression : given an image and a small neihborhood, the winner-take-all scheme can be applied to select the edges [6]. We will use the winner-take-all in order to select the direction of the line-process as we discuss in section 4.

3 Four line-process model :

The main drawback of all these models is to favor the detection of horizontal and vertical lines. This could be a problem according to the type of images to be analysed : if the goal is the detection of buildings or roads in an aerial image it can be sufficient (cf [35],[36]); but if the images are presenting diagonals or curves together with horizontal and vertical lines. it is better to use another model.

Now, we introduce line-processes in 4 directions. Calling $l^{n}_{i,j}$ the line-process which connects the site(i,j) to the site(i-1,j), $l^{nw}_{i,j}$ the one which connects the site(i,j) to the site(i-1,j-1), $l^{w}_{i,j}$the one which connects the site(i,j) to the site(i,j-1) and $l^{sw}_{i,j}$ the one which connects the site(i,j) to the site(i+1,j-1) (see Fig.2), an energy can be defined as follows :

$$E_1 = \sum_{i,j}[(y_{i,j} - d_{i,j})^2 + \alpha(\Delta^{sw\,2}_{i,j}(1 - l^{sw}_{i,j}) + \Delta^{nw\,2}_{i,j}(1 - l^{nw}_{i,j}) + \Delta^{n}_{i,j}{}^{2}(1 - l^{n}_{i,j}) + \Delta^{w}_{i,j}{}^{2}(1 - l^{w}_{i,j})) + \gamma(l^{sw}_{i,j} + l^{nw}_{i,j} + l^{n}_{i,j} + l^{w}_{i,j})] \quad (13)$$

where :

$$\Delta_{i,j}^{sw} = y_{i,j} - y_{i+1,j-1} \quad (14)$$
$$\Delta_{i,j}^{nw} = y_{i,j} - y_{i-1,j-1} \quad (15)$$
$$\Delta_{i,j}^{n} = y_{i,j} - y_{i-1,j} \quad (16)$$
$$\Delta_{i,j}^{w} = y_{i,j} - y_{i,j-1} \quad (17)$$

As previously, the energy is composed of 3 terms which stand for enforcing the closeness to the data, for smoothing the image and for a penalty cost to create an edge.

Using MF approximation, we get after some algebraic manipulations the following equations:

$$\begin{aligned} \bar{y}_{i,j} = d_{i,j} - \alpha[&\Delta_{i,j}^{\bar{n}}(1-\bar{l}_{i,j}^{n}) - \Delta_{i+1,j}^{\bar{n}}(1-\bar{l}_{i+1,j}^{n}) + \\ &\Delta_{i,j}^{\bar{w}}(1-\bar{l}_{i,j}^{w}) - \Delta_{i,j+1}^{\bar{w}}(1-\bar{l}_{i,j+1}^{w}) + \Delta_{i,j}^{n\bar{w}}(1-\bar{l}_{i,j}^{nw}) - \\ &\Delta_{i+1,j+1}^{n\bar{w}}(1-\bar{l}_{i+1,j+1}^{nw}) + \Delta_{i,j}^{s\bar{w}}(1-\bar{l}_{i,j}^{sw}) - \Delta_{i-1,j+1}^{s\bar{w}}(1-\bar{l}_{i-1,j+1}^{sw})] \end{aligned} \quad (18)$$

$$\bar{l}_{i,j}^{n} = \sigma_{\beta}(\alpha\Delta_{i,j}^{\bar{n}\,2} - \gamma) \quad (19)$$
$$\bar{l}_{i,j}^{w} = \sigma_{\beta}(\alpha\Delta_{i,j}^{\bar{w}\,2} - \gamma) \quad (20)$$
$$\bar{l}_{i,j}^{nw} = \sigma_{\beta}(\alpha\Delta_{i,j}^{n\bar{w}2} - \gamma) \quad (21)$$
$$\bar{l}_{i,j}^{sw} = \sigma_{\beta}(\alpha\Delta_{i,j}^{s\bar{w}2} - \gamma) \quad (22)$$

Once the convergence of the algorithm has been obtained, a winner-take-all scheme is used to select the edges. Basically, this is equivalent to have an additional layer above the lattice presented in Fig.2 where an edge at site(i,j) is defined by a scalar line-process $l_{i,j}$ given by :

$$l_{i,j} = \begin{cases} 1 & \text{if } max(l_{i,j}^{n}, l_{i,j}^{w}, l_{i,j}^{nw}, l_{i,j}^{sw}) > 0.5 \\ 0 & \text{otherwise} \end{cases}$$

4 Line-process propagation :

Furthermore, one can think to add a constraint in the energy function in order to propagate the lines. The idea is to use the original model (13) within the statistical and mean

field approach and lower the temperature to obtain a finer solution for the line-processes. However at low temperatures, i.e. after a first segmentation has been obtained, we start propagating the lines depending upon the line-process configuration. At this stage, the image y has already been stabilized. We propose to add to the model (13) the cost :

$$\begin{aligned} E_2 = E_1 - \xi \sum_{i,j} [& l^{nw}_{i,j}(1-l^{sw}_{i,j})(1-l^{sw}_{i-1,j+1})(l^{nw}_{i-1,j+1}+l^{nw}_{i+1,j-1}) + \\ & l^{sw}_{i,j}(1-l^{nw}_{i,j})(1-l^{nw}_{i+1,j+1})(l^{sw}_{i+1,j-1}+l^{sw}_{i-1,j-1}) + \\ & l^{n}_{i,j}(1-l^{w}_{i,j})(1-l^{w}_{i,j+1})(l^{n}_{i,j+1}+l^{n}_{i,j-1}) + \\ & l^{w}_{i,j}(1-l^{n}_{i,j})(1-l^{n}_{i+1,j})(l^{w}_{i+1,j}+l^{w}_{i-1,j})] \end{aligned} \tag{23}$$

Then, the price to be paid to create an edge at site(i,j) in the North-West direction, for example, will be :

$$l^{nw}_{i,j}[\gamma - \xi(1-l^{sw}_{i,j})(1-l^{sw}_{i-1,j+1})(l^{nw}_{i-1,j+1}+l^{nw}_{i+1,j-1})] \tag{24}$$

The term $(l^{nw}_{i-1,j+1} + l^{nw}_{i+1,j-1})$ enforces the propagation of the line, whereas the term $((1-l^{sw}_{i,j})(1-l^{sw}_{i-1,j+1}))$ avoids line propagation in the case of already existing perpendicular lines. ξ is a parameter which is equal to zero at high temperatures (i.e. low β) and which can be increased gently when the temperature goes to zero ($\xi \in [0,1]$) in order to propagate the lines only when one has a good confidence in the created lines.

Applying again the mean field techniques, we obtain the following mean field equations :

$$\bar{l}^{n}_{i,j} = \sigma_\beta(\alpha\Delta^{\bar{n}\,2}_{i,j} + \xi(1-\bar{l}^{w}_{i,j})(1-\bar{l}^{w}_{i,j+1})(\bar{l}^{n}_{i,j+1}+\bar{l}^{n}_{i,j-1}) - \gamma) \tag{25}$$

$$\bar{l}^{w}_{i,j} = \sigma_\beta(\alpha\Delta^{\bar{w}\,2}_{i,j} + \xi(1-\bar{l}^{n}_{i,j})(1-\bar{l}^{n}_{i+1,j})(\bar{l}^{w}_{i+1,j}+\bar{l}^{w}_{i-1,j}) - \gamma) \tag{26}$$

$$\bar{l}^{nw}_{i,j} = \sigma_\beta(\alpha\Delta^{\bar{nw}\,2}_{i,j} + \xi(1-\bar{l}^{sw}_{i,j})(1-\bar{l}^{sw}_{i-1,j+1})(\bar{l}^{nw}_{i-1,j+1}+\bar{l}^{nw}_{i+1,j-1}) - \gamma) \tag{27}$$

$$\bar{l}^{sw}_{i,j} = \sigma_\beta(\alpha\Delta^{\bar{sw}\,2}_{i,j} + \xi(1-\bar{l}^{nw}_{i,j})(1-\bar{l}^{nw}_{i+1,j+1})(\bar{l}^{sw}_{i-1,j-1}+\bar{l}^{sw}_{i+1,j+1}) - \gamma) \tag{28}$$

and for the image y the mean field equation is the same as (18).

We point out that other line propagation schemes have been suggested in [6], [7], for example. In [7] the problem is that they propagate horizontal lines if there are already horizontal lines and analogously for the vertical lines, but there is no mechanism to stop the propagation in the perpendicular direction. Therefore each diagonal line will propagate in both directions (horizontal and vertical) creating crosses!. The scheme in [6] will propagate lines in all the directions and again does not have a mechanism to stop the formation of crosses.

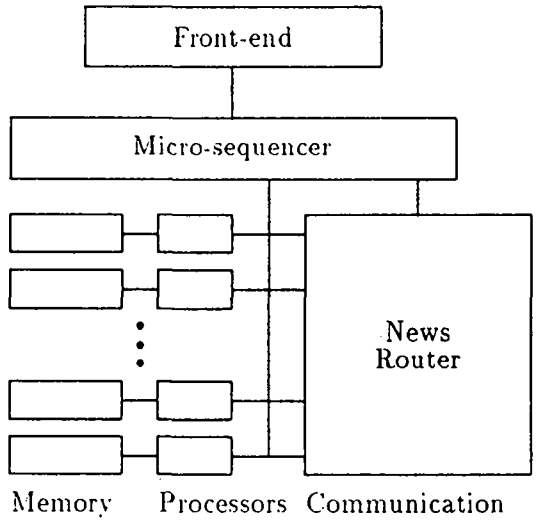

Figure 3: CM-2 architecture

5 Simulation :

5.1 Implementation on the CM2 :

In this section, we briefly describe the architecture of the Connection Machine (see Fig. 3), a more detailed description can be found in [13],[29].The Connection Machine is a single instruction multiple data (SIMD) parallel computer with 8K to 64K processors. Each processor is a 1-bit serial processor, with 32K bytes of local memory and a 8MHz clock. For a given application, the user can dynamically define a particular geometry for the set of physical processors that has been attached.

The processor resource can be virtualized when the number of data elements to be processed is greater than the number of physical processors. In such a case, several data elements are processed on a single physical processor. Such a data parallelism model architecture is well suited to computer vision as shown in [18], [31].

For the deterministic relaxation algorithms described in this paper, we use the data parallelism (one pixel per virtual processor) and the fast local communications (NEWS). For global operations like computing the energy value over the whole image, we use the reduce primitives.

Without entering into all the details of the algorithm implementation, we should men-

tion that the minimization of the energy for a given temperature has been done with an optimal step descent method for $\bar{y}$. A conjugate gradient algorithm (see [19] and [26] for more details about the Polak and Ribiere extension) has been chosen because this technique is known to be robust to noise [27],[37].

5.2 Choice of the parameters :

The parameters α, γ, ξ and the annealing on β have to be chosen in order to develop an algorithm which detects the discontinuities of a given data field :

- α corresponds to the regularization term which reflects the confidence we have in the data. therefore if the data are noisy, α is set high because of the low confidence in the data and it effects a great deal of smoothing.

- γ is the penalty to be paid to create an edge. When $\xi = 0$, a threshold h for creating the discontinuities can be exhibited :

$$h = \sqrt{\frac{\gamma}{\alpha}} \tag{29}$$

  This threshold defines the resolution of the system : when the gradient in one direction is greater than this threshold, a discontinuity is detected in this direction.

- ξ stands for the propagation parameter, it has to be zero at high temperatures and to increase gently when the detection is nearly sure ($\xi \in [0,1]$). We have chosen the following schedule :

$$\xi = \xi + \Delta\xi \tag{30}$$

  starting with $\xi = 0$.

- β is proportional to the inverse of a temperature. We have tried different schedules for annealing. We have found that the quality of the edge map is very dependent on this schedule : the slower it is, the better are the results. We currently use the following one :

$$\beta = \beta * 4 \tag{31}$$

starting with $\beta = 0.00005$ and doing 7 iterations for the annealing.

5.3 Simulation results :

For all the images, we have worked with free boundaries and have used the following initial conditions for a given temperature : the first time ($\beta = 0.00005$), we initialize $\bar{y}$ as the noisy data and the line-processes to zero. Then, we take as initial conditions the values of $\bar{y}_{i,j}, \bar{l}^{n}_{i,j}, \bar{l}^{w}_{i,j}, \bar{l}^{nw}_{i,j}, \bar{l}^{sw}_{i,j}$ obtained after convergence at the previous temperature.

First, we have tested the algorithm with very simple synthetic images (checkerboard, diagonal). Then, we have applied the method to real noisy images. We present the results obtained with two of them at the end of this paper. The first picture (256,256) is an Infra-Red aerial image (see Fig. 4). The edge map presented in Fig. 5 has been obtained with the following parameters : $\alpha = 2.0, \gamma = 30.0, \Delta\xi = 0.0$. The convergence has been obtained after 181 iterations. This result can be compared to the edge map obtained with the previous model with horizontal and vertical line-processes (see Fig. 6) with $\alpha = 6.0$, $\gamma = 180$ which are the most suitable parameters we have found for this algorithm. The curves of the road and some buildings are better detected with the proposed model. The second image (256,256) is a medical one (some fibers of a muscle, see Fig. 7), the result shown in Fig. 8 has been obtained with $\alpha = 2.0, \gamma = 150.0, \Delta\xi = 4.0$ after 238 iterations and can be compared with Fig. 9 given by the previous model with $\alpha = 6.0$, $\gamma = 300$. The contours of the fibers are more closed in Fig. 8 than in Fig. 9.

Finally, Table 1 gives the computational time necessary on the connection machine CM2 (using only 8 Kprocessors).

	VPR	CM time (s)	Total time (s)	Nber of it.	CM time per It.
Infra-Red	8	176.59	202.25	181	0.97
Muscle	8	228.20	237.56	238	0.96

Table 1 : Performances of the proposed algorithm on the CM2

6 Conclusion :

In this paper, we have proposed a new model using line-processes in 4 directions and a winner-take-all scheme in order to have a better detection of diagonal lines and curves. A deterministic relaxation algorithm using Mean Field Annealing has been derived. The results obtained on different types of images are improved compared to those got with the

previous model using only horizontal and vertical line-processes.

[0]The authors would like to thank Florimond Ployette for his help in testing the algorithms on the connection machine and the GdR 134 TdSI for providing the pictures presented in this paper.

7 References :

1. J. Besag, "On the statistical analysis of dirty pictures", *Jl of Roy. Statist. Soc., series B*, Vol. 68, pp 259-302, 1986.

2. G. Bilbro, R. Mann, T. Miller, W. Snyder, D. Van den Bout, M. White, "Optimization by mean field annealing", *Advances in Neural Information Processing Systems*, Touretzky Ed., Vol.1, pp 91-98, 1988.

3. A. Blake, "Comparison of the efficiency of deterministic and stochastic algorithms for visual reconstruction", *IEEE Trans. on PAMI*, Vol. 11, pp 2-12, 1989.

4. A. Blake, A. Zisserman, "Visual reconstruction", *MIT Press, Cambridge - MA*, 1987.

5. C. Campbell, D. Sherington, K.Y.M. Wong, "Statistical mechanics and neural networks", *"Neural Computing Architecture", MIT Press, Cambridge - MA*, I. Aleksander Ed., pp 239-257, 1989.

6. D. Geiger, A.L. Yuille, "A common framework for image segmentation", *Proc. ICPR*, pp 502-507, Atlantic City, NJ, Jun. 1990.

7. D. Geiger, F. Girosi, "Parallel and deterministic algorithms for MRFs : surface reconstruction and integration", *Proc. ECCV*, pp 89-98, Antibes, Apr. 1990.

8. D. Geiger, F. Girosi, "Mean field theory for surface reconstruction", *DARPA Image Understanding Workshop*, pp 617-630, Palo-Alto, CA, May 1989.

9. D. Geman, S. Geman, C. Graffigne, P. Dong, "Boundary detection by constrained optimization", *IEEE Trans. on PAMI*, Vol. 12, pp 609-628, 1990.

10. D. Geman, G. Reynolds, "Constrained restoration and the recovery of discontinuities", *Research report*, Dept. of Math. and Stat., Univ. of Mass., Jan. 1990.

11. S. Geman, D. Geman, "Stochastic relaxation, Gibbs distributions and the Bayesian restoration of images", *IEEE Trans. on PAMI*, Vol. 6, pp 721-741, 1984.

12. P. Herault, J. Niez, "How neural networks can solve hard graph problems : a performance study on the graph K-partitioning", *Proc. Neuro-Nimes*, pp 237-255, Nimes, Nov. 1989.

13. W.D. Hillis, "The Connection Machine ", *Cambridge, MA, MIT Press*, 1985.

14. F. C. Jeng, J. W. Woods, "Image estimation by stochastic relaxation in the compound gaussian case", *Proc. ICASSP*, pp 1016-1019, New-York, Apr. 1988.

15. R. Kindermann, J.L. Snell, "Markov random fields and their applications", *Amer. Math. Soc.*, Vol. 1, pp 1-142, 1980.

16. S. Kirkpatrick, C. Gelatt, M. Vecchi, "Optimization by simulated annealing", *Science 220*, pp 671-680, 1983.

17. C. Koch, J. Marroquin, A.L. Yuille, "Analog neural networks in early vision", *Proc. Natl. Acad. Sci. B83*, pp 4263-4267, 1986.

18. J. Little, G. Belloch, T. Cass, " Algorithmic techniques for computer vision on a fine-grain parallel machine", *IEEE Tmns. on PAMI*, Vol. 11, pp 244-257, 1989.

19. D. Luenberger, "Linear and nonlinear programming", *Addison Wesley, 2nd Edition*, 1984.

20. J. Marroquin, "Deterministic Bayesian estimation of Markovian random fields with applications to computational vision", *Proc. ICCV*, pp 597-601, London, Jun. 1987.

21. J. Marroquin, S. Mitter, T. Poggio, "Probabilistic solution of ill-posed problems in computational vision", *Jl Am. Stat. Assoc.*, Vol. 82, pp 76-89, 1987.

22. G. Parisi, "Statistical Field Theory", *Adisson Wesley*, 1988.

23. M. Plischke, P.B. Bergersen, "Equilibrium Statistical Physics", *Prentice Hall, Englewood Cliffs - NJ*, 1989.

24. T. Poggio, V. Torre, C. Koch, "Computational vision and regularization theory", *Nature*, Vol. 317, pp 314-319, 1985.

25. A. Rangarajan, R. Chellappa, "Generalised Graduated Non-Convexity algorithm for Maximum A Posteriori image estimation", *Proc. ICPR*, pp 127-133, Atlantic City, NJ, Jun. 1990.

26. T. Simchony, R. Chellappa, Z. Lichtenstein, "Pyramid implementation of optimal step conjugate search algorithms for some low level vision problems", *IEEE Trans. on SMC*, Vol. 19, pp 1408-1426, 1989.

27. T. Simchony, R. Chellappa, Z. Lichtenstein, "The Graduated Non Convexity algorithm for image estimation using Compound Gauss-Markov Field models", *Proc. ICASSP*, pp 1417-1420, Glasgow, May 1989.

28. D. Terzopoulos, "Regularization of ill-posed visual reconstruction problems involving discontinuities", *IEEE Trans. on PAMI*, Vol. 8, pp 413-424, 1986.

29. Thinking Machine Corporation, "Connection Machine, Model CM2 Technical Summary" *TMC, Cambridge, MA*, May 1989.

30. P.J. Van Laarhoven, E.H. Aarts, "Simulated annealing : Theory and applications", *Reidel Pub., Dordrecht, Holland*, 1987.

31. H. Voorhees, D. Fritzsche, L. Tucker, "Exploiting data parallelism in Vision on the Connection Machine system", *Proc. ICPR*, Atlantic City, NJ, Jun. 1990.

32. A.L. Yuille, "Generalized deformable models, statistical physics and matching problems", *Neural Computation*, Vol. 2, pp 1-24, 1990.

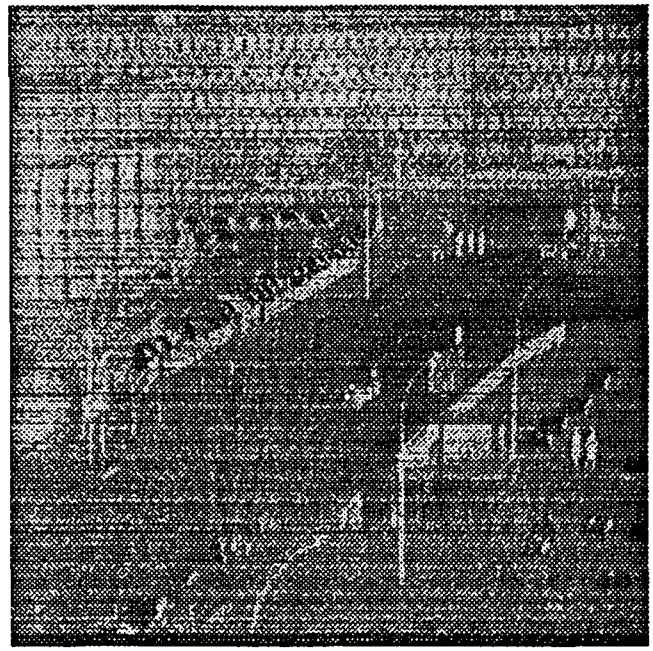

Fig 4: Original IR image

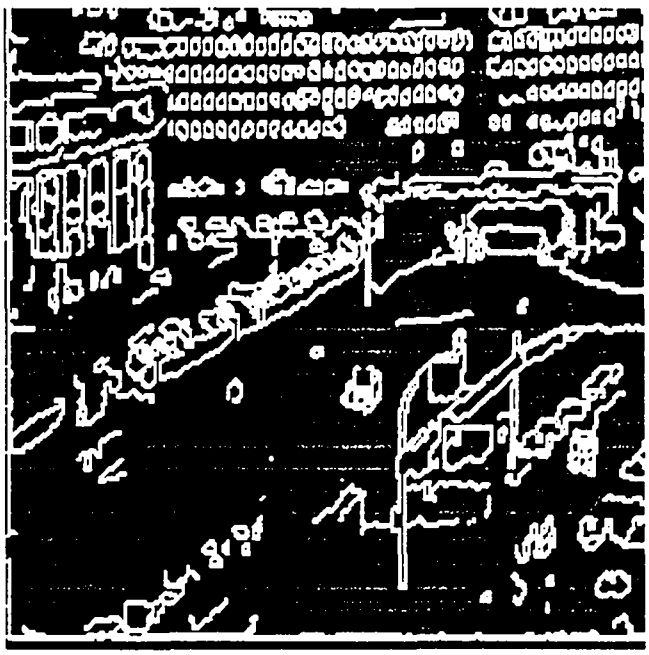

Fig 5: Edge map using 4 dir. line-processes

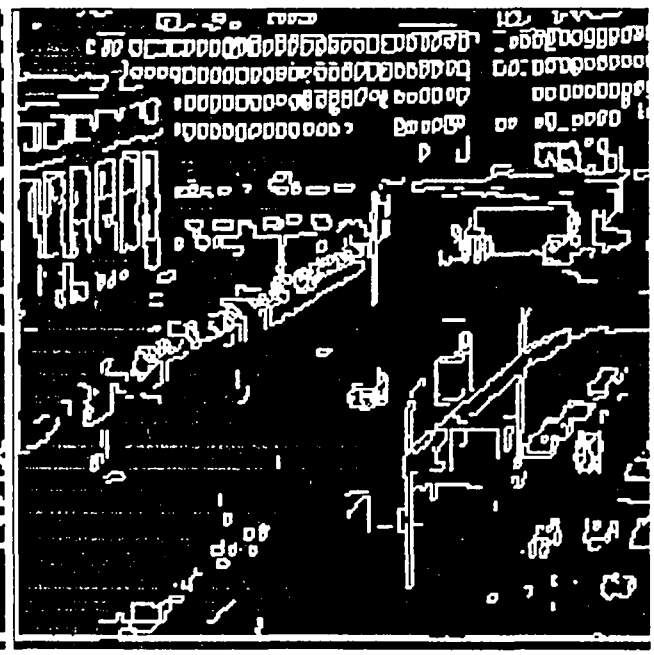

Fig 6: Edge map using horizontal and vertical line-processes

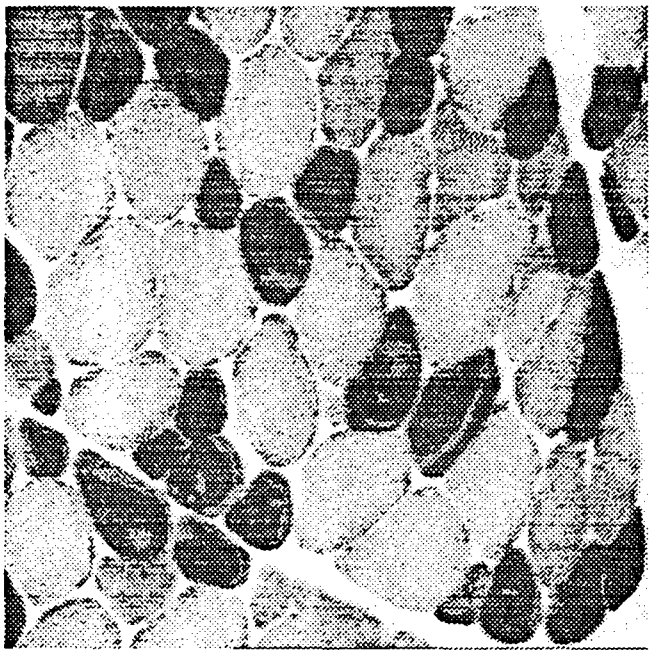

Fig 7: Image of muscle fibers

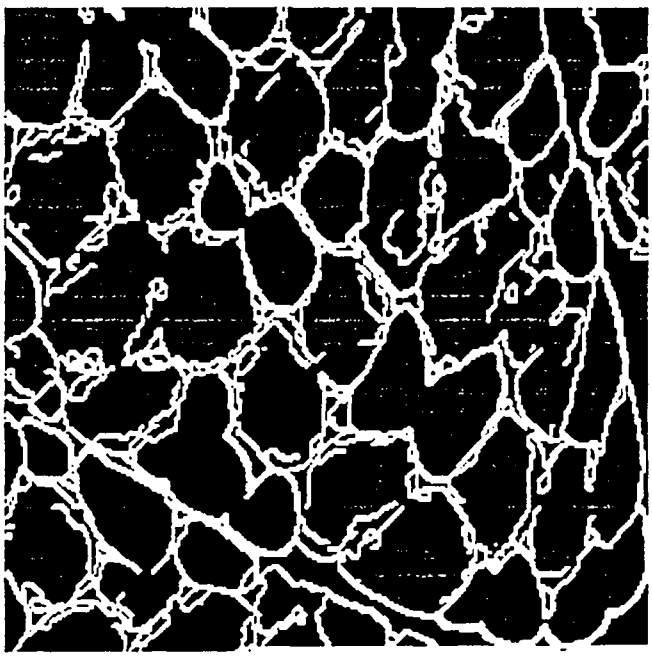

Fig 8: Edge map using 4 dir. line-processes

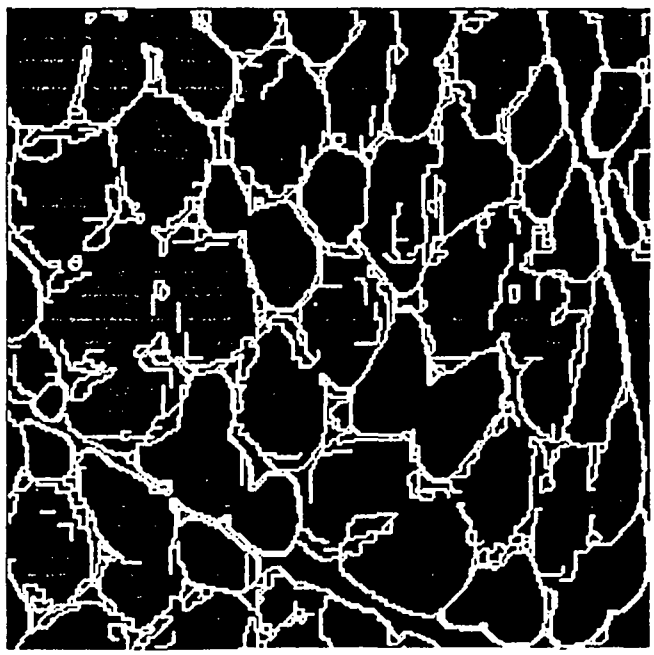

Fig 9: Edge map using horizontal and vertical line-processes

Imprimé en France
par
. l'Institut National de Recherche en Informatique et en Automatique

ISSN 0249-6399